Conductive Inks with a "Built-In" Mechanism That Enables Sintering at Room Temperature

Michael Grouchko,[§] Alexander Kamyshny,[§] Cristina Florentina Mihailescu,[‡] Dan Florin Anghel,[‡] and Shlomo Magdassi[§,*]

[§]Casali Institute for Applied Chemistry, Institute of Chemistry, The Hebrew University of Jerusalem, Jerusalem 91904, Israel and [‡]Colloid Department, Ilie Murgulescu Institute of Physical Chemistry, 060021 Bucharest, Romania

ABSTRACT At present there is no metallic ink that enables formation of conductive patterns at room temperature by a single printing step. Printing conductive features by metallic nanoparticle-based inks must be followed by sintering while heating to elevated temperatures, thus preventing their utilization on most plastic substrates used in plastic electronics. In this report we present a new silver nanoparticle-based conductive ink, having a built-in sintering mechanism, which is triggered during drying of the printed pattern. The nanoparticles that are stabilized by a polymer undergo self-sintering spontaneously, due to the presence of a destabilizing agent, which comes into action only during drying of the printed pattern. The destabilizing agent, which contains Cl^- ions, causes detachment of the anchoring groups of the stabilizer from the nanoparticles' surface and thus enables their coalescence and sintering. It was found that the new metallic ink leads to very high conductivities, by a single printing step: up to 41% of the conductivity of bulk silver was achieved, the highest reported conductivity of a printed pattern that is obtained from nanoparticles at room temperature.

KEYWORDS: silver nanoparticles · plastic electronics · sintering · conductive printing

At present there is no metallic ink that enables formation of conductive patterns at room temperature by a single printing step. Printing conductive features, for example in plastics electronics[1,2] by metallic nanoparticle inks, must be followed by an additional step of sintering, usually achieved by heating to elevated temperatures.[3−5] In this step, the nanoparticles (NPs) composing the pattern will coalesce to form a continuous electrical contact.[5] New sintering processes such as microwave[4,6] or laser radiation,[7] xenon flash light,[8] electrical[9] or chemical sintering,[10] and plasma[11] have been developed; however, these processes involve high-cost equipment and require high energy or complex pre- or post-treatments. Therefore, there is an unmet need for inks that will lead to high electrical conductivity once printed and will not require an additional sintering step.

In this report we present a new concept for conductive inks that contain a built-in sintering mechanism. Instead of carrying out the sintering as an additional sequential step after printing the metallic NPs, we suggest a new dispersion that can self-sinter spontaneously once it dries on the substrate. This dispersion is mainly a dispersion of electrosterically stabilized silver NPs, together with a low concentration of a destabilizer, which acts as a sintering agent and comes into action only upon drying of the dispersion. The sintering agent, which can be a simple electrolyte such as NaCl, destabilizes the silver nanoparticles and leads to their close contact. The chloride ions replace and detach the anchoring groups of the polymeric stabilizer from the nanoparticles' surface and thus enable their coalescence and sintering. It was found that such a process leads to very high conductivities, up to 41% of the conductivity of bulk silver, the highest reported conductivity of a printed pattern that is obtained at room temperature.

RESULTS AND DISCUSSION

As illustrated in Figure 1, the destabilization concept involves the spontaneous removal of the polymeric stabilizer from the NPs' surface upon drying the dispersion, thus leading to their contact and coalescence. In this work we used silver NPs with an average diameter of 15 nm, stabilized by polyacrylic acid sodium salt (PAA Na), synthesized as described previously.[10] In order to trigger the polymer desorption, we first explored its adsorption mechanism. As can be seen from the SERS spectra of a diluted Ag NPs dispersion (0.025 wt % Ag) presented in Figure 2a, the strongest SERS peaks are at 1391, 855, and 229 cm^{-1}, which can be attributed to the $\nu_s O-C-O$, $\nu_s C-C$, and $\nu Ag-OCO^-$ bands, respectively,[12,13]

* Address correspondence to magdassi@cc.huji.ac.il.

Received for review February 13, 2011 and accepted March 25, 2011.

Published online March 25, 2011
10.1021/nn2005848

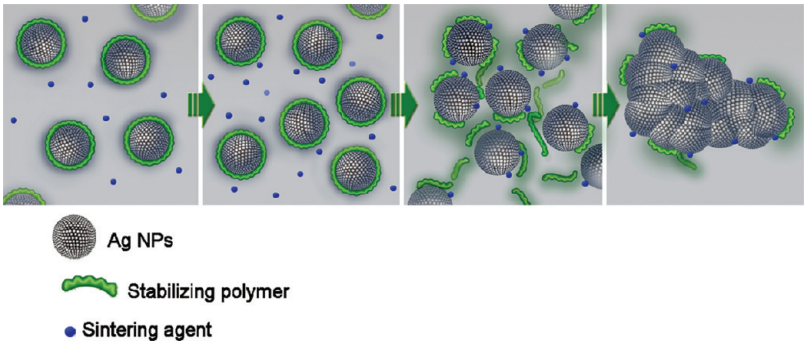

Figure 1. Schematic illustration of the stabilizer detachment, which leads to the NP sintering (the green lines represent the polymeric stabilizer; the blue spheres represent the sintering agent).

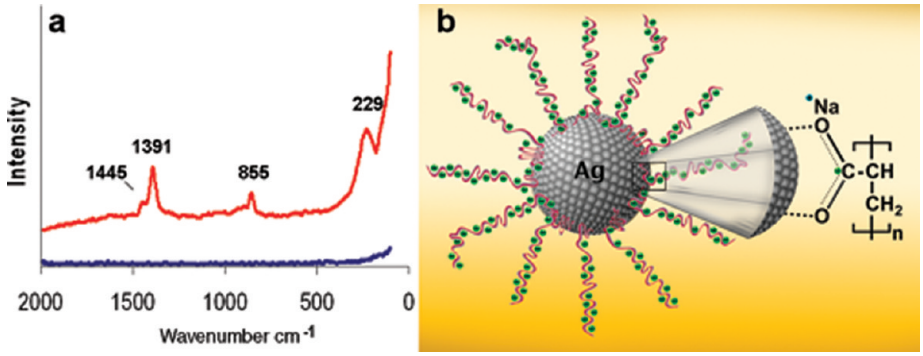

Figure 2. (a) Raman spectra of Ag NPs stabilized by PAA Na (red, upper spectrum) and the same polymer without Ag NPs (blue, lower spectrum) and (b) a schematic illustration of the PAA Na adsorbed to the NP surface.

These peaks indicate clearly that the main interaction of the polymer with the Ag surface is through the carboxylic group, namely, by Ag−O interaction (the moderate 855 cm^{-1} peak indicates that there is also an interaction through the hydrophobic part of the polymer). According to FTIR spectra of free PAA Na compared with that PAA Na adsorbed on the Ag NPs, the $\Delta\nu_{poly}$ and $\Delta\nu_{ads}$ (referring to the difference between the symmetric and asymmetric stretching of the carboxylate group of the free polymer, ν_{poly}, and the adsorbed polymer, ν_{ads}, respectively) are quite close, 152 and 154 cm^{-1}, respectively (Supporting Information Figure S1). These close values indicate that the carboxylate anchors to the Ag NPs' surface through a bidentate mode,[14] probably by ion−dipole interactions. Figure 2b illustrates the binding mode of the polymeric stabilizer to the surface of silver NPs.

Therefore, desorption of the polymer requires detachment of the carboxylate group from the Ag surface. Such desorption may be possible by replacing the carboxylate with another moiety at the same site. Since halides are known to have very strong interactions with silver, various halides (LiCl, NaF, NaCl, NaBr, NaI, KCl, $MgCl_2$, $CaCl_2$, $AlCl_3$, NH_4Cl, and HCl) were evaluated as "desorbing agents" for PAA from the Ag NPs surface. In this report we will concentrate on the effect of NaCl and HCl on the desorption of PAA from Ag NPs and how it triggers the spontaneous sintering of the NPs even at room temperature.

Figure 3a presents the SERS spectra of Ag NP dispersion containing NaCl at various concentrations. It can be clearly seen that as the NaCl concentration increases, the 1391 cm^{-1} (ν_sOCO) and 855 cm^{-1} (ν_sCC) bands decrease while the 229 cm^{-1} (νAg−OCO$^-$) peak increases dramatically and shifts to 247 cm^{-1} (the drastic change occurs above 50 mM NaCl). As illustrated in Figure 3b, we suggest that these changes result from the replacement of the carboxylate (Ag−OCO$^-$) by a chloride (Ag−Cl$^-$), which leads to the desorption of the polymer (while the Na^+ ions serve as the counterions).[15−18] Direct evidence for this desorption mechanism was achieved by using a fluorescently labeled PAA Na (pyrene:carboxylic 1:305 molar ratio). It was found by fluorescence measurements that once NaCl is added to the NP dispersion, the polymer is desorbed from the NPs (Supporting Information Figure S2). Figure 3c presents the consequential effect of the desorption of the polymeric stabilizer on the size of the particles in the dispersion (evaluated by dynamic light scattering). It was found that a drastic increase in the average particle size occurs, from ∼15 nm to 0.2−6 μm. Characterization of these large particles by HR-SEM (Supporting Information Figure S3) remarkably reveals that the increase in particle size is due to the coalescence of the particles and not simply due to aggregation of the NPs.

This sharp transfer from individual nanoparticles (up to 50 mM NaCl) to coalesced nanoparticles (above

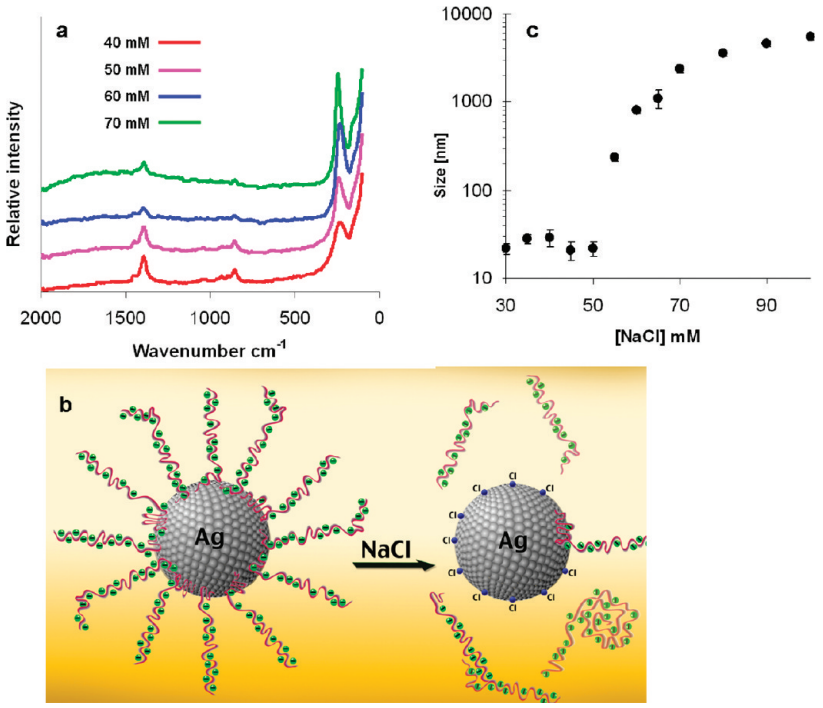

Figure 3. (a) SERS spectra of Ag NPs with increasing NaCl concentration, (b) schematic illustration of the NP before (left) and after (right) the addition of NaCl, and (c) average particle size measured by dynamic light scattering as a function of NaCl concentration.

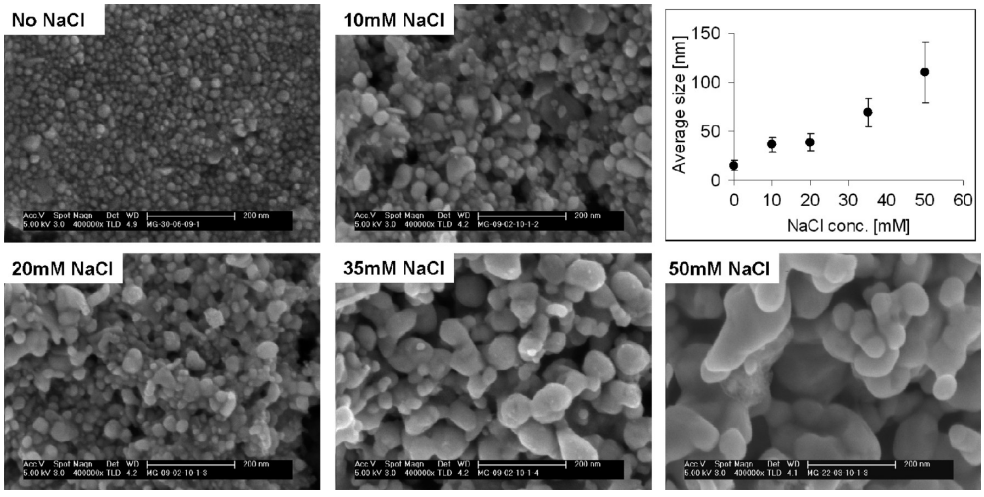

Figure 4. HR-SEM images of the dried Ag NP dispersion on PET with increasing NaCl initial concentration and the obtained average particle size as a function of NaCl concentration.

50 mM NaCl) was implemented to achieve self-sintering of the silver NPs, which is triggered only upon printing. Once the dispersion is printed, evaporation of the dispersion medium (water) takes place, and this causes the inevitable increase of NaCl concentration. Therefore, while starting with a low NaCl concentration in the dispersion (which does not cause significant desorption of the stabilizer) the dispersion is stable prior to printing. After evaporation of the water, the salt concentration increases and leads to desorption of the stabilizing polymer and eventually to sintering of the nanoparticles. Indeed, as seen in the HR-SEM images of the dried dispersions on poly(ethylene terephthalate) (PET) in Figure 4, increasing the initial NaCl concentration increases the degree of sintering and particle size, resulting in an interconnected network. Conductive atomic force microscope (C-AFM) measurements indeed confirm the formation of a continuous network that is electrically conductive. The increase in the number of percolation paths as the NaCl concentration increases is evident; see Supporting Information Figure S4.

A deeper investigation of the obtained network is obtained by combining SEM and TEM observations

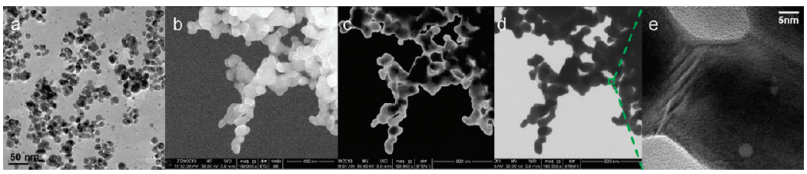

Figure 5. (a) TEM image of the NPs with no NaCl, (b) SEM, (c) dark field TEM, and (d) bright field TEM images of the Ag NPs with 20 mM NaCl, and (e) HR-TEM magnification of the necks formed at the same [NaCl].

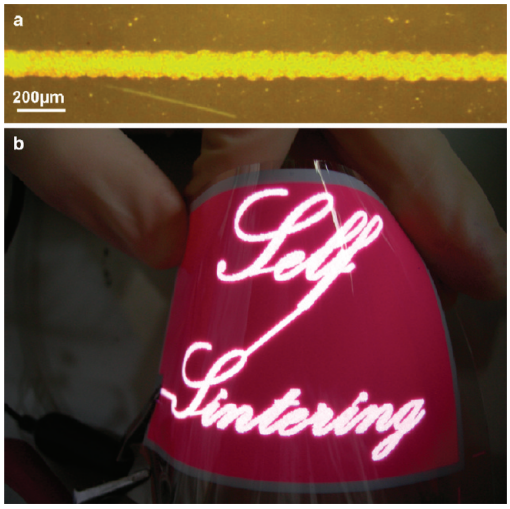

Figure 6. (a) Inkjet-printed line (the dispersion contained 20 wt % silver and 50 mM NaCl) on PET film and (b) EL device printed with the same dispersion composition.

(Figure 5). It can be seen that the stabilized NPs without NaCl (Figure 5a) are characterized by an average particle size of 15(±5) nm and are nicely separated when dried. However, while drying a dispersion with initial low concentration of NaCl (20 mM) at room temperature, there are no free NPs since all particles were sintered together (Figure 5b−d). As can be seen in the TEM images (Figure 5c and d), and especially in the HR-TEM high-magnification image (Figure 5e), necks are formed due to coalescence of the particles, which forms a continuous metallic network. Figure 5e shows as well that these necks are characterized by lattice mismatches, probably due to the coalescence of particles with different lattice orientations, which occurs at low temperature, and does not allow optimization of the lattice structure.

The stability of the silver dispersion at low NaCl concentration ([NaCl] < 50 mM) enabled testing the "self-sintered" dispersion as a conductive inkjet ink. Conductive patterns were formed by printing on flexible plastic substrates without the need for any postprinting sintering process (the sintering takes place at room temperature during the water evaporation). Figure 6a presents a line printed on PET (width 95 μm and thickness 0.5 μm) with a resistivity of 16(±2.2) $\mu\Omega$cm, which is as low as 10 times that of bulk silver. As presented in Figure 6b, this "self-sintering" process, which occurs even at room temperature, enabled the

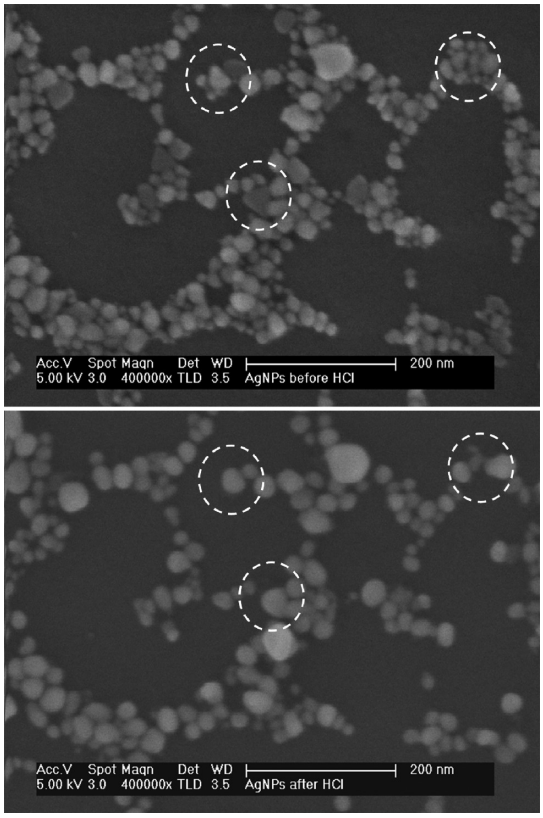

Figure 7. HR-SEM images of the same zone (a) before (up) and (b) after (down) exposure to HCl vapor.

fabrication of an electroluminescent (EL) plastic device (Figure 6b) with no need for postprinting heating to elevated temperature. This result is of great importance for printing on heat-sensitive materials and opens new avenues in plastics-printed electronics.

It should be noted that the conductivity of the self-sintered silver pattern was about 10% that of bulk silver. This is due to the well-sintered particles, but could be improved if a denser packing of the nanoparticles was obtained.

The low-density packing of the nanoparticles (Supporting Information Figure S5) is a result of the immediate coalescence of the NPs in the liquid, which does not enable any optimization of the packing. In order to achieve denser packing but still use the same destabilization process (with Cl^- ions), the two processes, destabilization and packing of the particles, should be separated. First a dense structure should be obtained due to evaporation of the water, and then the

closely packed NPs should be sintered. Obviously, treatment of a dried silver NP array by a NaCl solution will lead to destruction of the obtained packing. In order to overcome this problem, we used a different source of Cl^- ions—HCl vapors—which do not destroy the dense packing. In this case the destabilization mechanism may involve as well the protonation of the PAA^- to PAAH, leading to loss of electrical repulsion between the nanoparticles. The coalescence under HCl vapors without significant destruction of the packing was verified by HR-SEM imaging of silver NPs (Figure 7). As shown, exposure to HCl vapors leads to disappearance of the small particles due to merging with the larger ones, indicating that the metallic NPs actually act as "soft material". A similar experiment was conducted with a more densely packed layer (which was obtained from a dispersion containing 20 wt % silver). It was found that the silver network obtained after 10 s exposure to HCl vapors is obviously much denser and has more percolation paths than the one obtained by NaCl (Supporting Information Figure S5).

This observation is reflected in a dramatic increase in the conductivity, 41% that of bulk silver (resistivity of 3.84 $\mu\Omega$cm). This result is the highest reported conductivity of a printed pattern that is obtained at room temperature. For comparison, such conductivity for the same dispersion can be obtained only after heating to 320 °C for 30 min.

In summary, we achieved a new "self-sintered" metal dispersion in which the sintering is triggered by changes in concentration of chloride ions. The sintering results from detachment of the anchoring groups of the stabilizing polymer from the NP surface.

It was found that this process enables close contact of the particles and leads to their sintering even at room temperature; thus the metallic nanoparticles actually behave as soft material. This approach leads to very high conductivities, up to 41% of the conductivity of bulk silver, the highest reported conductivity of structures obtained at room temperature. We expect that these findings will open new avenues in direct printing of conductive features in printed devices and especially in plastic electronics.

EXPERIMENTAL SECTION

Ag NP Synthesis. The silver NPs were synthesized by the reduction of silver acetate with ascorbic acid in the presence of PAA Na (MW = 8000) as described previously.[10] The pyrene-labeled NPs were synthesized by the same procedure but while replacing 10 wt % of the PAA Na by the same quantity of the pyrene-labeled PAA Na (MW = 25 000). The labeled PAA Na 25 000 was obtained from the pyrene-labeled poly(acrylic acid) (PAAH) by neutralization with NaOH. The labeled polymer was synthesized from the corresponding PAAH (Wako, Japan) according to a previously described procedure.[19] The quantity of chromophore incorporated was determined from the ultraviolet (UV) absorption data of polymer solutions in methanol using as a model 1-pyrenylmethylamine hydrochloride (ε_{342} = 37 500 L mol^{-1} cm^{-1} in methanol). The UV measurements revealed that, on average, 1 pyrene group corresponds to 305 acrylic acid monomer units (~1.1 pyrene per macromolecule).

Exposure to HCl Vapor. The printed substrates were placed 2 cm above a 37% HCl solution for 10 s.

Characterization Methods. HR-SEM and TEM images were obtained with a Sirion (FEI) scanning electron microscope, and XHR Maggellan 400 L (FEI). HR-TEM images were obtained with a high-resolution TEM, Tecnai F20 G^2 (FEI). The C-AFM measurements were carried out by a Nanoscope Dimension 3100 (Digital Instruments). The dynamic light scattering particle size measurements were carried out by a Zetasizer ZS (Malvern).

The SERS spectra were taken using a Nicolet NXR 9650 Raman spectrometer (Thermo Scientific) with a 1064 nm laser, the FTIR spectra by an Alpha (Bruker), and fluorescence spectra by an Eclipse fluorescence spectrophotometer (Cary) under excitation at 355 nm. The resistivity of printed patterns was calculated by measuring the printed line resistance by a milliohm meter (EXTECH) and measuring the cross-sectional profile of the pattern by the use of a Veeco Dektak 150+ surface profiler.

Inkjet Composition and Printing. The silver dispersion printed by a Dimatix DMP 2800 inkjet printer was composed of 20 wt % silver nanoparticles, 10 wt % propylene glycol (Merck), and 0.05 wt % BYK 348 (BYK Chemie). The pattern printed as electrodes on the EL device was printed by the use of the same formulation by a Lexmark Z615 office printer. The four-layer (PET/ITO/ZnS/$BaTiO_3$) EL device was fabricated by MOBIChem Scientific Engineering. Then, the self-sintered silver ink was printed on top of the $BaTiO_3$.

Acknowledgment. This research was supported by the European Community's Seventh Framework Programme, through Collaborative Project LOTUS, Project Number 248816, and by the SES Magnet Program of the Israel Trade and Industry Ministry. We also thank Prof. Y. Haas and A. Kahan for the FT-Raman characterization. The authors would also like to thank Dr. Inna Popov and the unit for nanocharacterization for the electron microscopy characterization.

Supporting Information Available: Additional figures. This material is available free of charge *via* the Internet at http://pubs.acs.org.

REFERENCES AND NOTES

1. Forrest, S. R. The Path to Ubiquitous and Low-Cost Organic Electronic Appliances on Plastic. *Nature* **2004,** *428*, 911–918.
2. Sirringhaus, H.; Kawase, T.; Friend, R. H.; Shimoda, T.; Inbasekaran, M.; Wu, W.; Woo, E. P. High-Resolution Inkjet Printing of All-Polymer Transistor Circuits. *Science* **2000,** *290*, 2123–2126.
3. Ahn, B. Y.; Duoss, E. B.; Motala, M. J.; Guo, X.; Park, S.; Xiong, Y.; Yoon, J.; Nuzzo, R. G.; Rogers, J. A.; Lewis, J. A. Omnidirectional Printing of Flexible, Stretchable, and Spanning Silver Microelectrodes. *Science* **2009,** *323*, 1590–1593.
4. Perelaer, J.; de Gans, B. J.; Schubert, U. S. Ink-Jet Printing and Microwave Sintering of Conductive Silver Tracks. *Adv. Mater.* **2006,** *18*, 2101–2104.
5. Sivaramakrishnan, S.; Chia, P. J.; Yeo, Y. C.; Chua, L. L.; Ho, P. K. H. Controlled Insulator-to-Metal Transformation in Printable Polymer Composites with Nanometal Clusters. *Nat. Mater.* **2007,** *6*, 149–155.
6. Perelaer, J.; Klokkenburg, M.; Hendriks, C. E.; Schubert, U. S. Microwave Flash Sintering of Inkjet-Printed Silver Tracks on Polymer Substrates. *Adv. Mater.* **2009,** *21*, 4830–4834.

7. Ko, S. H.; Pan, H.; Grigoropoulos, C. P.; Luscombe, C. K.; Frechet, J. M. J.; Poulikakos, D. Air Stable High Resolution Organic Transistors by Selective Laser Sintering of Ink-Jet Printed Metal Nanoparticles. *Appl. Phys. Lett.* **2007,** *90*, 141103–141103−3.
8. Kim, H. S.; Dhage, S. R.; Shim, D. E.; Hahn, H. T. Intense Pulsed Light Sintering of Copper Nanoink for Printed Electronics. *Appl. Phys. A: Mater. Sci. Process.* **2009,** *97*, 791–798.
9. Allen, M. L.; Aronniemi, M.; Mattila, T.; Alastalo, A.; Ojanpera, K.; Suhonen, M.; Seppa, H. Electrical Sintering of Nanoparticle Structures. *Nanotechnology* **2008,** *19*, 175201.
10. Magdassi, S.; Grouchko, M.; Berezin, O.; Kamyshny, A. Triggering the Sintering of Silver Nanoparticles at Room Temperature. *ACS Nano* **2010,** *4*, 1943–1948.
11. Reinhold, I.; Hendriks, C. E.; Eckardt, R.; Kranenburg, J. M.; Perelaer, J.; Baumann, R. R.; Schubert, U. S. Argon Plasma Sintering of Inkjet Printed Silver Tracks on Polymer Substrates. *J. Mater. Chem.* **2009,** *19*, 3384–3388.
12. Arenas, J. F.; Castro, J. L.; Otero, J. C.; Marcos, J. I. SERS of Acrylic Acid and Methyl Derivatives on Silver Sols. *J. Raman Spectrosc.* **1998,** *29*, 585–591.
13. Ooka, A. A.; Kuhar, K. A.; Cho, N. J.; Garrell, R. L. Surface Interactions of a Homologous Series of Alpha, Omega-amino Acids on Colloidal Silver and Gold. *Biospectroscopy* **1999,** *5*, 9–17.
14. Kirwan, L. J.; Fawell, P. D.; van Bronswijk, W. In situ FTIR-ATR Examination of Poly(acrylic acid) Adsorbed onto Hematite at Low pH. *Langmuir* **2003,** *19*, 5802–5807.
15. Chen, S. H.; Ren, X. M. SERS Studies of Methylviologen on Silver Sol and the Effect of Halide-Ions. *Spectrochim. Acta, Part A* **1995,** *51*, 717–725.
16. Wetzel, H.; Pettinger, B.; Wenning, U. Surface-Enhanced Raman-Scattering from Ethylenediaminetetraacetic-Disodium Salt and Nitrate Ions on Silver Electrodes. *Chem. Phys. Lett.* **1980,** *75*, 173–178.
17. Pergolese, B.; Muniz-Miranda, M.; Bigotto, A. Surface Enhanced Raman Scattering Investigation of the Halide Anion Effect on the Adsorption of 1,2,3-Triazole on Silver and Gold Colloidal Nanoparticles. *J. Phys. Chem. B* **2005,** *109*, 9665–9671.
18. Liang, E. J.; Engert, C.; Kiefer, W. Surface-Enhanced Raman-Scattering of Halide-Ions, Pyridine and Crystal Violet on Colloidal Silver with near-Infrared Excitation−Low-Wave-Number Vibrational-Modes. *Vib. Spectrosc.* **1995,** *8*, 435–444.
19. Anghel, D. F.; Alderson, V.; Winnik, F. M.; Mizusaki, M.; Morishima, Y. Fluorescent Dyes as Model Hydrophobic Modifiers' of Polyelectrolytes: a Study of Poly(acrylic acid)s Labelled with Pyrenyl and Naphthyl Groups. *Polymer* **1998,** *39*, 3035–3044.